Probabilistic Mesomechanics for High Cycle Fatigue Life Prediction

Robert G. Tryon
Thomas A. Cruse
Fellow ASME
Brentwood Technologies, Inc.,
Brentwood, TN 37027

This paper presents an analytical modeling approach to characterize and understand high cycle fatigue life in gas turbine alloys. It is recognized that the design of structures subjected to fatigue cannot be based on average material behavior but that designs must consider -3σ or some other appropriate extreme value (tail of the distribution) loading and/or material properties. Thus, a life prediction capability useful in a design application must address the scatter inherent in material response to fatigue loading. Further, the life prediction capability should identify the key micromechanical variables that are critical in the tail of the materials durability distribution. The proposed method addresses the scatter in fatigue by investigating the microstructural variables responsible for the scatter and developing analytical and semi-analytical models to quantitatively relate the variables to the response. The model is general and considers the entire range of damage accumulation sequences; from crack nucleation of the initially unflawed structure to final fast fracture. [S0094-4289(00)01302-5]

Introduction

Many material and structural design factors influence component reliability in terms of the defined durability problems. From a material performance standpoint, many of these factors are at work in the durability ''size effect.'' Two important aspects of the size effect influence high cycle fatigue (HCF) in mechanical components: the relative size of the stressed area compared to the size of the component and the relative size of the damage (crack) compared to the size of the microstructure.

The size effect was first reported by Peterson [1] when he noticed that the mean fatigue life and variation in fatigue life were a function of the stressed volume. The size effect must be carefully considered in regards to HCF of such components as aeroengine airfoils. The stresses that cause HCF are often mode shapes bending stresses induced by vibratory excitation. Only a very small portion of the total airfoil area is subjected to the high stresses.

The size effect has another fundamental role in controlling HCF because damage accumulation often starts on a small scale. HCF failures are not usually initiated by the large microstructural defects associated with low cycle fatigue failures but often nucleate ''naturally'' at local regions of high stress. The local regions of high stress may be caused from vibratory resonance or foreign object damage. The damage grows through various mechanisms, including crack nucleation, microstructurally small crack growth, and linear elastic long crack growth. Each mechanism is associated with a characteristic size and each characteristic size has its own geometric complexities, constitutive laws and heterogeneities. Fatigue behavior cannot be fully understood and predicted without obtaining information about each of the characteristic sizes, or what can be called mesodomains. Nested models can link each of the mesodomains to determine the response of the macrodomain.

The overall fatigue response of a component is predicted by nesting the individual mesoscale models. The lowest level model uses the appropriate mesoscale parameters to determine the initial state of the next level. This level uses the results from the previous level along with the appropriate parameters to determine the initial state of the next level and so on. Using nested models, fleet reliability can be linked to the heterogeneities at each mesodomain. Additionally, by modeling each level of the fatigue process individually, and rigorously linking the levels, various size effects are included.

Three Level Fatigue Model

Figure 1 shows the three levels of damage accumulation that are assumed in the present study. First, the crack nucleates on a small scale on the order of the grain size. Then the crack grows as a microstructurally small crack in which the crack front lies in relatively few grains. The material properties, averaged along the crack front, approach bulk material properties as the crack grow and the number of grains interrogated by the crack front increase. At this point, linear elasticity can be assumed and the crack grows as a typical long crack until final failure.

The models used to predict the behavior for each of the three levels of damage accumulation have been discussed elsewhere [2] and only those aspect of the models related to HCF of gas turbine alloys will be discussed.

Crack Nucleation Model. Models used in the research must have two attributes. They must be quantitative with regards to the number of cycles needed to produce a crack to a specific size if they are to be used for lifetime predictions. The models must also be able to address the microstructural parameters in order to provide a physical link between the microstructure and the fatigue behavior. The crack nucleation model used in the current research addresses slip band cracking within a grain that is a preferred mode of damage accumulation for HCF in gas turbine alloys [3]. The model used in this effort is based on a model proposed by Tanaka and Mura [4] and extended to account for grain orientation by Tryon and Cruse [3] as

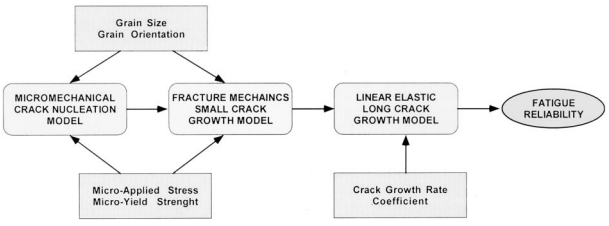

Fig. 1 Three-stage mesomechanical fatigue model

Contributed by the Materials Division for publication in the JOURNAL OF ENGINEERING MATERIALS AND TECHNOLOGY. Manuscript received by the Materials Division June 23, 1998; revised manuscript received November 1, 1999. Associate Technical Editor: H. Sehitoglu.

$$N_n = \frac{4GW_s}{\left(\frac{1}{M_S}\Delta\sigma - 2k\right)^2 \pi(1-\nu)d} \tag{1}$$

where N_n is the number of cycles needed to grow a crack to the size of the grain, G is the shear modulus, W_s is the specific fracture energy per unit area, σ is the local applied normal stress, M_S is grain orientation factor (reciprocal Schmid factor), k is the frictional stress which must be overcome to move dislocations, υ is Poissons ratio, and d is the grain diameter.

Small Crack Growth Model. The behavior of small cracks differs from the behavior of long cracks. Long crack behavior can be predicted using conventional continuum based LEFM techniques. Small crack growth rates vary widely, from several orders of magnitude greater than that predicted by continuum based ΔK to complete arrest. A small crack can be thought of as a crack with a size on the order of the microstructure. The anomalous growth of small cracks has been attributed to two competing factors: high growth rates due to lack of closure and growth retardation due to microstructural obstacles.

Crack Tip Opening Displacement. The experimentally observable parameter that has been correlated to the varying small crack growth rate is the crack tip opening displacement (CTOD) [5]

$$\frac{da}{dN} = C'\Delta\phi_t \tag{2}$$

where a is the crack length, N is cycles, ϕ_t is the CTOD, and C' is a material constants derived from test data. The CTOD is a measure of the amount of damage associated with the crack tip. The larger the CTOD, the higher the crack growth rate. This phenomenon was first observed by Laird and Smith [6] and has been well established in long crack growth behavior [7]. The direct proportionality of Eq. (2) has been observed in small crack growth of aluminum, nickel and titanium alloys [8]. Nisitani and Takao [9] showed that small crack arrest could be associated with zero CTOD.

In the current research, the CTOD is modeled as a function of the random microstructural variables based on the approach used by Tanaka et al. [10] and extended by Tryon [2]. Consider a crack of length a with the crack tip in the jth grain as shown in Fig. 2. The slip band has a length of w with the slip band tip in the nth grain. The total length of the damage, c, is the crack length plus the slip band length. If the slip band is propagating (not blocked by the grain boundary), the size of the slip band zone can be found from

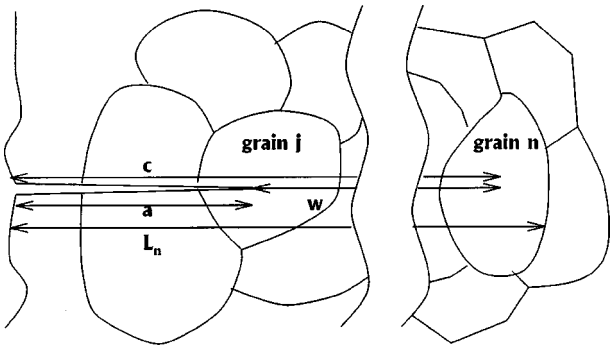

Fig. 2 Crack tip slip band in multiple grains

$$0 = \frac{\pi\tau_j}{2} - k_j \arcsin\frac{a}{c} - \sum_{i=j+1}^{n} [(\tau_{i-1} - k_{i-1}) - (\tau_i - k_i)] \arcsin\left(\frac{L_{i-1}}{c}\right) \tag{3}$$

where, τ_i is the applied resolved shear stress in the ith grain, k_i is the frictional stress of the ith grain, a is the crack length, c is the crack length plus slip band length, L_i is the distance from the free surface to grain boundary of the ith grain preceding the slip band tip as shown in Fig. 2.

The CTOD is given by

$$\phi_t = \frac{2k_j a}{\pi^2 A}\ln\frac{c}{a} + \sum_{i=j+1}^{n} \frac{(\tau_{i-1} - k_{i-1}) - (\tau_i - k_i)}{\pi^2 A} g(a;c,L_{i-1})$$

$$g(a;c,L) = L\ln\left|\frac{\sqrt{c^2-L^2}+\sqrt{c^2-a^2}}{\sqrt{c^2-L^2}-\sqrt{c^2-a^2}}\right| - a\ln\left|\frac{a\sqrt{c^2-L^2}+L\sqrt{c^2-a^2}}{a\sqrt{c^2-L^2}-L\sqrt{c^2-a^2}}\right| \tag{4}$$

$$A = G/2\pi(1-\nu) \quad \text{for edge dislocations}$$

$$A = G/2\pi \quad \text{for screw dislocations}$$

For the slip band blocked by the grain boundary, the size of the slip band zone is

$$\omega = L_n - a \tag{5}$$

The CTOD is given by

$$\phi_t = \frac{\beta\tau}{\pi A}\sqrt{c^2-a^2} + \frac{2k_j a}{\pi^2 A}\ln\frac{c}{a} + \sum_{i=j+1}^{n} \frac{(\tau_{i-1} - k_{i-1}) - (\tau_i - k_i)}{\pi^2 A} g(a;c,L_{i-1})$$

$$\beta = 1 - \frac{2k_j}{\pi\tau_j}\arccos\frac{a}{c} - \sum_{i=j+1}^{n} \frac{2[(\tau_{i-1} - k_{i-1}) - (\tau_i - k_i)]}{\pi\tau_j}\arccos\left(\frac{L_{i-1}}{c}\right) \tag{6}$$

The microscopic stress intensity factor at the slip band tip is

$$K_m = \beta\tau\sqrt{\pi c} \tag{7}$$

To account for the crystallographic orientation of the individual grains, the applied resolved shear stress τ in Eqs. (3) through (7) can be replaced with

$$\tau = \frac{\sigma}{M_S} \quad \text{for surface grains}$$

$$\tau = \frac{\sigma}{M_T} \quad \text{for interior grains}$$

where σ is the local normal applied stress, M_S is the reciprocal Schmid factor and M_T is the Taylor factor [12].

Modeling the Physical Microstructure

Consider a random array of grains as shown in Fig. 3. A crack nucleates in the surface grain X_0 and then grows along the x axis as a semi-circle through zones in which the effective material properties are uniform. The boundaries of the zones are represented by the concentric half circles. The zones are composed of grains represented by the semi-circular arc segments. The arc length of the semi-circular segments is a random variable equal to the grain diameter. The surface grains are represented by the in-

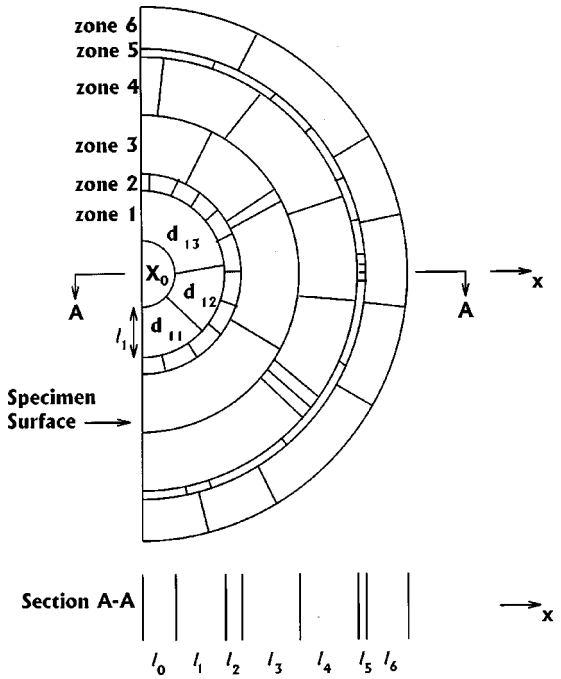

Fig. 3 Array of random grains

tersection of the zones and the surface. Note that because the crack grows as a semi-circle, the surface crack growth is the same as the in-depth crack growth through the zones represented by Section A-A.

After successful crack nucleation, the crack grows from grain X_0 into zone 1. In the example shown in Fig. 3, zone 1 contains three grains. The effective material property $P_{1\,\mathrm{eff}}$, of zone 1 is the average of the properties of the individual grains.

P_{1i} weighted with the area of the ith grain. (In the current study $P_{1\,\mathrm{eff}}$ represents the local frictional strength k or the local applied stress τ.)

$$P_{1\,\mathrm{eff}}=\frac{P_{11}d_1^2+P_{12}d_{12}^2+P_{13}d_{13}^2}{d_1^2+d_{12}^2+d_{13}^2} \tag{8}$$

In the nth zone composed of j grains, the effective material property is

$$P_{n\,\mathrm{eff}}=\frac{\Sigma_{i=1}^{j}P_{ni}d_{ni}^2}{\Sigma_{i=1}^{j}d_{ni}^2} \tag{9}$$

As the crack becomes long, $P_{n\,\mathrm{eff}}$ approaches the bulk properties.

Using the concepts of effective material properties, crack growth is modeled as one-dimensional. Consider a cut along the x axis (Section A-A in Fig. 3). The fatigue damage is modeled as a one-dimensional crack growing through zones of varying size l_n and varying effective material properties $P_{n\,\mathrm{eff}}$.

The above microstructural modeling technique is approximate and does not capture some of the nuances of crack/microstructure interactions. In particular, the model does not allow for spatial variation of properties along the crack front that can cause a non-smooth or ragged crack front shape. If the crack front encounters strong grains (due to unfavorable orientation or high frictional stress) in a matrix of weaker grains, the crack front will retard in the region near the strong grains and tunnel in the region of the weak grains. However, crack growth mechanisms tends to have a smoothing effect on the crack front shape. The crack front will tunnel around the blockage until the shape of the crack front at the blockage is such that the stress intensity overcomes the blockage and the crack front resumes its smooth shape [11]. If the blockage is not overcome, the crack front will not continue to tunnel. The crack growth will arrest.

Long Crack Growth Model. The long crack growth is modeled using the Paris law representation of a surface crack in a semi-infinite body subjected to a constant stress cycle. If the final crack size is much greater than the initial crack size, Tryon and Cruse [12] showed that

$$N_g=\frac{a_i^{1-n/2}}{C\Delta\sigma^n\beta^n\left(\frac{n}{2}-1\right)} \tag{10}$$

where, N_g is the number of cycles needed for the crack to grow to failure, a_i is the initial crack size at the start of the long crack growth phase, $\Delta\sigma$ is the global stress range, β is the geometry constant (1.12π), and C and n are based on material properties.

Monte Carlo Simulation Model

The statistical characteristics of variables used in the Monte Carlo simulation have been discussed in detail in Tryon and Cruse [13]. The random variables and the associated statistical distributions are shown in Table 1. Normalized distributions are used for d, a, k, and C. This allows the average values to be easily changed without having to re-evaluate the distribution parameters. The distribution parameters only need to be re-evaluated if a change in coefficient of variation (COV) is desired. The orientation factors are not normalized. A change in the average value of the orientation factor would require texturing the microstructure. The values

Table 1 Values used in the Monte Carlo simulation

Variable	Description	Distribution type	Distribution Parameters		Average	COV
C	Paris Law Coefficient	Lognormal	$\lambda=0.034$	$\zeta=0.30$	4.4×10^{-9} MPa$\sqrt{m}$	0.30
C'	CTOD Law Coefficient	Deterministic	N/A		0.10	N/A
d	Grain diameter	Lognormal	$\lambda=-0.076$	$\zeta=0.39$	55.8 μm	0.40
da	Small Crack Growth Interval	Deterministic	N/A		0.5	N/A
G	Bulk Shear Modulus	Deterministic	N/A		76×10^{-3} MPa	N/A
k	Frictional Strength	Weibull	$\eta=1.12$	$\zeta=3.7$	69 MPa	0.30
K_{crit}^{M}	Critical Microstructural Stress Intensity Factor	Deterministic	N/A		769 MPa$\sqrt{m}$	N/A
M_S	Schmid Orientation Factor	Curve Fit (See Ref. [12])			2.21	0.08
M_T	Taylor Orientation Factor	Curve Fit (See Ref. [12])			3.07	0.13
n	Paris Law Exponent	Deterministic	N/A		3	N/A
W_S	Specific Fracture Energy	Deterministic	N/A		440 kN/m	N/A
ν	Poisson's Ratio	Deterministic	N/A		0.3	N/A
σ	Applied Micro-stress	Normal	$\mu=1$	$\sigma=0.3$	Variable*	0.30

*Note: Several different stress levels are modeled as discussed in the Section on Model Results.

in Table 1 would no longer be valid and new representations would be required. The deterministic input variables are also shown in Table 1.

The basic flow of the Monte Carlo simulation is outlined as follows. A crack is nucleated in each surface grain of a component. Each crack goes through the small crack growth phase and long crack growth phase. The total life associated with each crack is the summation of the cycles in the crack nucleation, small crack growth and long crack growth phases. The life of the component is equal to the minimum total life of all of the cracks. The details of the simulation are described in Tryon [2].

Model Results

The predictions of the individual crack nucleation, small crack growth, and long crack growth simulations have been shown to correlate very favorably with experimental observations and are discussed elsewhere [3,12]. In this section, we will discuss the prediction of the total fatigue life for a simple test specimen.

Predicted Total Fatigue Life of a Test Specimen. It is difficult to compare the probabilistic model predictions for total fatigue life directly with experimental data because the parameters used in the model are usually not reported. However, the predicted scatter in fatigue data is compared with trends in the experimental data and the predicted mean life for different size specimens is compared with size effect observations.

The distribution of fatigue life for test specimens was predicted by assuming the parameters in Table 1 in the Monte Carlo analysis. These values are characteristic of a stainless steel. The specimen has a circular cross section with radius 7.62 mm, and a shallow notch with a gauge surface area of 1.61 mm^2. This gauge surface area results in about 4000 grains per specimen. Different specimens will have a different number of surface grains and therefore the number of surface grains is a random variable. The predicted CDF of fatigue life for the specimens is shown in Fig. 4. The mean life of the specimens is 60,000 cycles with a COV of 0.17.

Figure 4 shows that fitting the model results to a lognormal distribution give a correlation coefficient of 0.993. Fitting the model results to a normal distribution (not shown) gives a correlation coefficient of 0.999. Both the normal and lognormal distributions provide an adequate representation of the model results and both have been used to represent experimental data [14,15], p. 380].

A thorough investigation of the scatter in fatigue life is not available in the literature for most alloys. Many manufacturers, particularly in the aerospace industry, have the large compilation

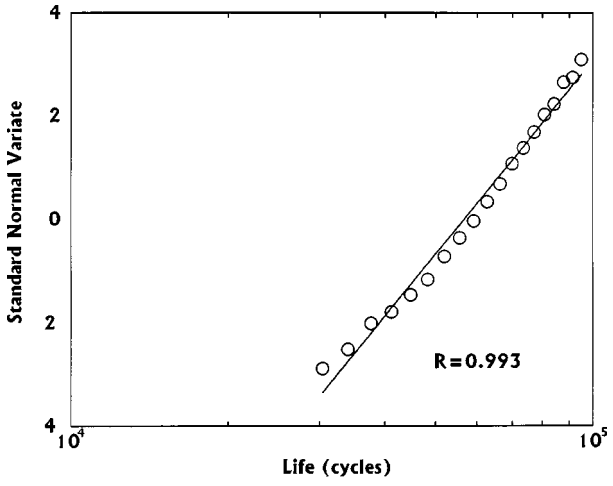

Fig. 4 Fatigue life distribution of the specimens plotted on lognormal probability paper

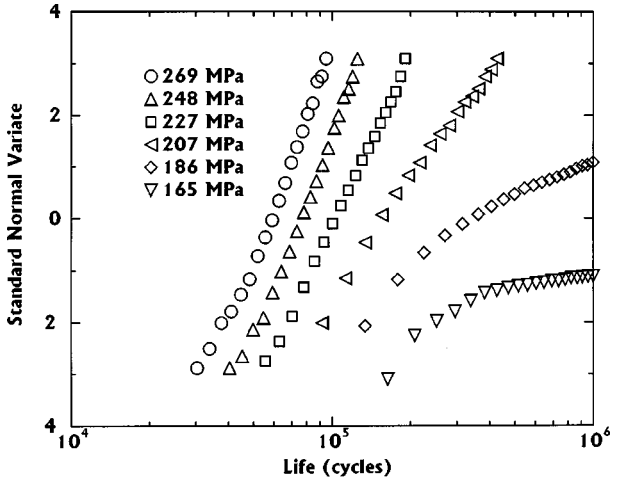

Fig. 5 Predicted fatigue life distribution plotted on lognormal paper

of data used for statistical characterization. However, the cost associated with such test is considerable and the data is tightly held. However, Bastenaire [14] performed a thorough investigation of the scatter in fatigue life for five different grades of low alloy steel.

Steels may nucleate cracks by mechanisms other than slip band cracking depending on the alloy composition and the impurities. However, the trend in the scatter in steel data has been observed in other metallic alloys [16]. Bastenaire performed rotating bending fatigue experiments for many stress levels for each grade of steel with several hundred specimens for each stress level.

Figure 6 shows the trends in the scatter exhibited in Bastenaire's data plotted on lognormal paper. (The curves are replotted from the data in Fig. 7 of [14].) If data plots as a straight line in Fig. 6, the lognormal distribution is valid. If data plots as a nonstraight line in Fig. 6, the lognormal distribution is no longer valid. The general trend is that the COV (indicated by the slope of the curves) is fairy constant for applied stresses well above the fatigue limit (363–324 MPa). As the applied stress decreases, the COV starts to increase (304–285 MPa). As the applied stress approaches the fatigue limit, the fatigue life increases and run-outs start to occur. The right tail of the distribution becomes more heavily populated than a lognormal distribution, which causes a line through the data to bend to the right (265–245 MPa). The 363 MPa data curves slightly to the left indicating the right tail of distribution is less populated than a lognormal distribution and the data can also be fitted to the normal distribution. As the applied stress decreases, the curvature shifts to the right.

Comparison of Fig. 5 with the results in Fig. 6 shows that the model predicts all of the above trends observed in the experimental data. Figure 7 presents the same data in the familiar form of a SN diagram. The runouts (suspensions) are the percentage of specimens that did not fail at 10^6 cycles.

The Monte Carlo simulation showed that most of the failures were caused by the largest grain in the specimen and almost all the failures were initiated in one of the five largest grains. The lower the stress the more failures initiated in the largest grain. This indicates that the ''weak links'' in crack nucleation are the largest grains. Experimental evidence shows that failures can be associated with the largest grains [11].

The distribution of the largest defects (or the largest grains in the present model) lead to the size effect model developed by Weibull [17]. Size effect is the phenomenon that small components have a higher fatigue life than larger geometrically similar components. Weibull assumed that the larger component is more

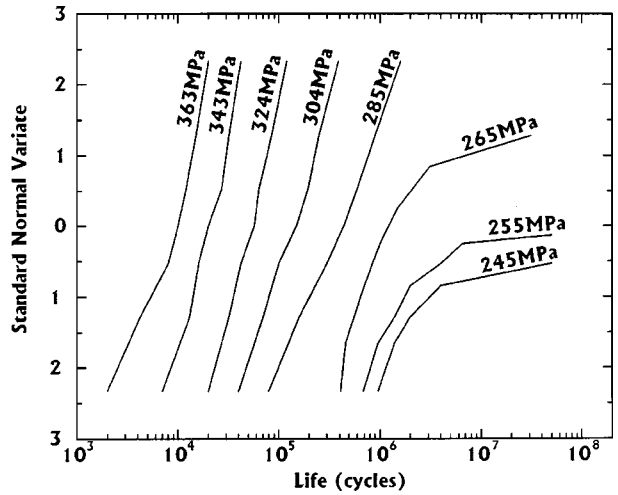

Fig. 6 Fatigue life test data plotted on lognormal paper (data from Bastenaire)

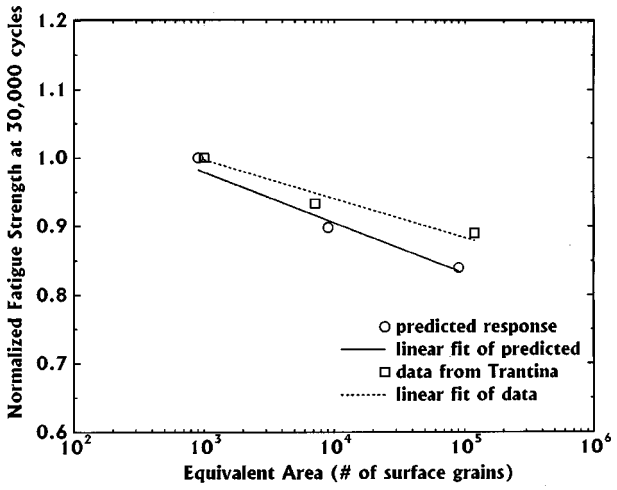

Fig. 8 Predicted stress versus life curve

likely to have a larger life-controlling defect. This approach is widely used in the design of ceramics and it has also been applied to ductile materials [18].

The reliability of different size (defined by the mean number of surface grains) specimens was determined and the mean fatigue strength at an arbitrary life is plotted against size in Fig. 8. The model indicates that very large structures have zero life. This is because a lognormal distribution of grains allows an infinitely large grain in an infinite population. In reality, the grain size cannot be infinite and the true distribution of grain size is truncated at a size no larger than the component. Maximum truncated grain size would control the fatigue life of a very large structure.

The predicted size effect on fatigue strength is linear in log space as shown in Fig. 8. Trantina [18] predicted the same relationship using a weakest link theory. Trantina's experimental observations on smooth, bolt hole and sharp notched specimens have been scaled with respect to fatigue strength for comparison with the model predictions in Fig. 8. A direct comparison cannot be made because the data exhibited is for a different material than that modeled. The important point demonstrated by Fig. 8 is that the model predicts that the fatigue life decreases linearly with an increase in the log of volume (or surface area). The intercept of the line depends on the specified fatigue life. The slope of the line, which represents the sensitivity of the material to size effect, depends on the scatter of the fatigue strength controlling variables and can vary with material processing and material alloy [18].

Sensitivities. The sensitivities shown in Figure 9 represent the sensitivity of the total fatigue life COV to the random variable COV.

To change in total life COV a Monte Carlo simulation was performed using the nominal variations in Table 1. Then a separate Monte Carlo simulation was performed for each of the random variables in which the COV the random variable was decrease by 5 percent. The sensitivities have been normalized such that the summation of sensitivities is one.

Figure 9 shows that at low stress (high cycle fatigue), the variation in fatigue life is most sensitive to the variation in the grain orientation. It is well known that texturing can greatly effect high cycle fatigue life. The variation in high cycle fatigue life is shown to be least sensitive to the variation in grain size. The Monte Carlo simulation showed that at low stress, the largest grains were responsible for the failure-causing crack. It would seem that the fatigue life would be sensitive to the grain size distribution. However, the distribution of the largest grains in each specimen is an extreme-value distribution and will only change slightly with a 5 percent decrease in the COV of grain size for all of the grains in the specimen.

Figure 9 shows that at high stress (low cycle fatigue), the variation in fatigue life is most sensitive to the variation in the applied

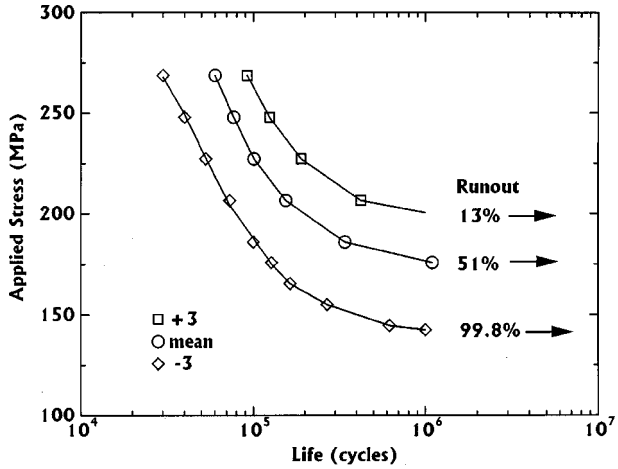

Fig. 7 Predicted mean fatigue life for various size specimens

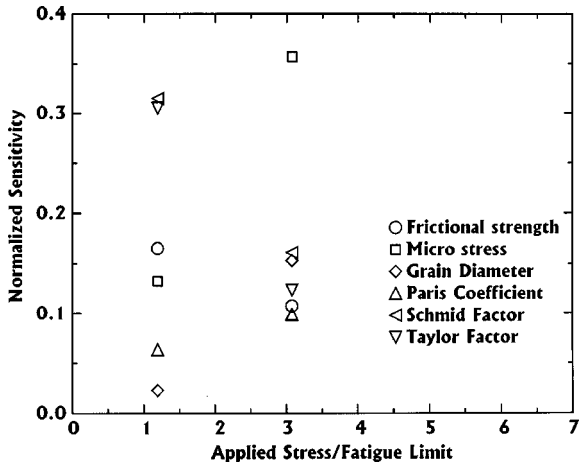

Fig. 9 Importance of the random variable variation on the fatigue life variation

microstress. In low cycle fatigue, the crack tip plastic zone is large and not as sensitive to the local material property variations. The scatter in fatigue life is more sensitive to grain size variations in low cycle fatigue than in high cycle. This is because the failure-causing crack is less likely to be associated with the largest grain in the specimen. The distribution for the entire population of grain size in the specimen will effect the failure causing cracks in low cycle fatigue. High cycle fatigue is a function of the extreme value distribution of grain size.

Summary

This study develops a probabilistic mesomechanical fatigue model to relate the variation in the material microstructure to the variation in the fatigue life of macrostructural components. Only the microstructural effects were investigated. Variations in the applied loading, stress concentrations, residual stresses, and global geometry are not considered.

Single-phase polycrystalline components are modeled. Grain shape is assumed equiaxial and the grain orientation is untextured. Loading and material properties within a grain are homogeneous although not isotropic and vary from grain to grain. Component geometries are simple smooth test specimens.

The fatigue process is divided into three phases. The first phase is the crack nucleation phase. The second phase is the small crack growth phase. Local microstructural variables considered random are grain size, grain orientation, micro-stress and frictional stress. The variables are common to both the crack nucleation and small crack growth models. The third phase is the long crack growth phase. Long crack growth rate is modeled using Paris law and microstructural variations are not explicitly considered. All variation in long crack growth is model by allowing the Paris law coefficient to be a random variable.

The model predicted many aspects of fatigue observed in the experimental data. These include:

- The shape of the total fatigue life distribution.
- The applied global stress effects on the shape of the total fatigue life distribution.
- The knee in the SN curve and run-outs.
- The size effect.

This study demonstrates the feasibility of developing probabilistic mesomechanical material models that can link the variation in the material microstructure to the scatter in fatigue life.

Acknowledgments

This work was supported by NASA SBIR Contract NAS 399040, Dr. P. L. N. Murthy, Technical Representative, and GSRP Project No. NGT-51053, Glenn Research Center, Dr. C. C. Chamis, Technical Advisor.

References

[1] Peterson, R. E., 1939, ''Methods of Correlating Data from Fatigue Test of Stress Concentration Specimens,'' *Contributions to the Mechanics of Solids*, Macmillan, pp. 179–183.
[2] Tryon, R. G., 1996, ''Probabilistic Mesomechanical Fatigue Model,'' Ph.D. thesis, Vanderbilt University.
[3] Tryon, R. G., Cruse, T. A., 1998, ''A Reliability-Based Model to Predict Scatter in Fatigue Crack Nucleation Life,'' Fatigue Fract. Eng. Mater. Struct., **21**, pp. 257–267.
[4] Tanaka, K., Mura, T., 1981, ''A Dislocation Model for Fatigue Crack Initiation,'' ASME J. Appl. Mech., **48**, pp. 97–103.
[5] Chan, K. S., Lankford, J., 1983, ''A Crack Tip Strain Model for the Growth of Small Fatigue Cracks,'' Scr. Metall., **17**, pp. 529–532.
[6] Laird, D., Smith, G. C., 1962, ''Crack Propagation in High Stress Fatigue,'' Philos. Mag., **7**, pp. 847–857.
[7] Weertman, J., 1979, ''Fatigue Crack Propagation Theories,'' Fatigue and Microstructure, ASM, Metals Park, Ohio, pp. 279–206.
[8] Hicks, M. A., Brown, C. W., 1984, ''A Comparison of Short Crack Growth Behavior in Engineering Alloys,'' Fatigue 84, Engineering Materials Advisory Services Ltd., England, pp. 1337–1347.
[9] Nisitani, H., and Takao, K-I., 1981, ''Significance of Initiation, Propagation and Closure of Microcracks in High Cycle Fatigue of Ductile Metals,'' Eng. Fract. Mech., **15**, No. 3, pp. 445–456.
[10] Tanaka, K., Kinefuchi, M., and Yokomaku, T., 1992, ''Modelling of Statistical Characteristics of the Propagation of Small Fatigue Cracks,'' Short Fatigue Cracks, Miller, K. J., and de los Rios, E. R., eds., ESIS 13, Mechanical Engineering Publications, London, pp. 351–368.
[11] Forsyth, P., 1969, The Physical Basis of Metal Fatigue, American Elsevier Publ., New York.
[12] Tryon, R. G., Cruse, T. A., 1997, ''Probabilistic Mesomechanical Fatigue Crack Nucleation Model,'' ASME J. Eng. Mater. Technol., **19**, No. 1, pp. 65–70.
[13] Tryon, R. G., Cruse, T. A., 1995, ''Probabilistic Mesomechanical Fatigue Crack Initiation Model, Phase 1: Crack Nucleation,'' ASME/JSME Pressure Vessel and Piping Conference, Honolulu, HI, Published in PVP-95-MF2.
[14] Bastenaire, F. A., 1972, ''New Method for the Statistical Evaluation of Constant Stress Amplitude Fatigue-Test Results,'' Probabilistic Aspects of Fatigue, Ed., Heller, R. A., ASTM STP 511, pp. 3–28.
[15] Dieter, G. E., 1986, *Mechanical Metallurgy*, McGraw-Hill, Third Edition.
[16] Sasaki, S., Ochi, Y., Ishii, A., Hirofumi, A., 1989, ''Effects of Material Structures on Statistical Scatter in Initiation and Growth Lives of Surface Cracks and Failure Life in Fatigue,'' JSME Inter. J., Series I, **32**, No. 1, pp. 155–161.
[17] Weibull, W., 1961, *Fatigue Testing and Analysis of Results*, Pergamon Press.
[18] Trantina, G., 1981, ''Statistical Fatigue Failure Analysis,'' J. of Test. Eval., **9**, No. 1, DD. 44–49.